B2 / PS3

LIMITING WINDSTORM EFFECTS ON TOWER BY A "LOW DRAG" CONDUCTOR

Jean-Louis LILIEN* Dmitri SNEGOVSKI	Thierry CAPELLE	Marc LE DU
UNIVERSITY OF LIEGE (Belgium)	NEXANS-BENELUX N. V. (Belgium)	EDF R&D (France)

Hurricane winds affect the flow around electrical conductor in a way that it may reach the critical (Drag crisis) and postcritical states. It is thus important to introduce the cable aerodynamic drag as Reynolds-dependent when calculating the response of the power transmission line under hurricane. To represent the respective wind loading on cable, the turbulent, spatially non-uniform wind model is used. In order to assess the behaviour and cyclic fatigue loads under hurricane conditions of different transmission line conductors, the time response analyses were done. Results of comparative study of the smooth cable AERO-Z and classical multistrand cable, including the percentage of load reduction offered to supporting structure, are presented.

Keywords: overhead transmission line, hurricane wind, smooth conductor, tower loading, fatigue effects

1. INTRODUCTION

According to Eurocode, in many European coastal areas the 50-year return winds reach the mean velocity 30 m/s and beyond [7], [13]. These statistics are supported by last years' observations: in 1998, 1999, 2002 and 2003 mean hurricane velocities up to 25 m/s near the ground were recorded. Needless to say what hard consequences such an event may bring on the ground structures. One of main concerns to the power transmission line is the wind turbulence-induced buffeting which, giving rise to the high-level dynamic loads, dramatically affects both PTL conductors and the towers.

When analysing the power transmission line's (PTL) response to hurricane, whole methodology follows the general rules in civil engineering, established in [2], [11] with account of conductor span nonlinearity. The key elements are correct modelling of structural aerodynamic plus an adequate model of wind. The response is assessed on basis of time-domain analysis [10], using an adequate method (either multibody or, as in our case, finite-element strategy) for nonlinear problem resolution.

The particular aspect of hurricane is that at such wind velocities the conductors are subject to the *critical* state of flow, marked by strong variations of drag coefficient. Being different on stranded and smooth conductors, the surface roughness significantly influences the character of drag variation on wind velocity (more precisely, on Reynolds number, $\mathcal{R}e$).

* lilien@montefiore.ulg.ac.be

2. CABLE AERODYNAMICS

Given ρ the air density (kg/m^3), D the diameter of conductor (m), and C_D the drag coefficient, the aerodynamic load per conductor's unit length is defined by expression:

$$F_D = \frac{\rho V^2}{2} D C_D \qquad \text{(N/m)} \qquad (1)$$

Here, the instant wind velocity V (m/s) is found from the relationship

$$\mathbf{V} = \mathbf{U} - \mathbf{V}_c \qquad (2)$$

where

$\mathbf{V}_c$ is the vector of relative cable velocity (m/s);

$\mathbf{U}$ is the vector of the wind velocity (m/s), defined after the model described below.

In our study we assessed the response of a smooth conductor Aero-Z (with Z-shaped fully locked strands) in comparison to the reference classical conductor, ASTER. Two conductors have close diameters (Aero-Z: 31.5 mm and Aster: 31.05 mm). Their wind tunnel test data on $C_D(\mathcal{R}e)$, compared to the purely smooth cylinder curve, are shown in Fig. 1. The stranding, the interstrand gaps imply the surface roughness which may significantly reduce the threshold for critical state. That is why both classical and smooth conductors reach the drag crisis within the levels of hurricane wind velocities.

The roughness of cable's surface is normally estimated by relationship k/h (here, k is the roughness characteristic size, and h is the conductor's diameter). For Aero-Z $k/h \sim 0.005$, and for Aster $k/h \sim 0.02$. As result, classical conductor reaches drag crisis at U = 15…20 m/s already. In the same time, decrease of its C_D in the critical state is quite shallow. The smooth conductor, Aero-Z, is closer to the purely smooth cylinder both in sense of the rate of drag fall and the $\mathcal{R}e$ level. In terms of wind velocities, the critical state of smooth conductor takes place at hurricane (U = 30…40 m/s). Here, given the deeper fall in C_D, drag crisis should significantly influence the aerodynamic loading of smooth conductor.

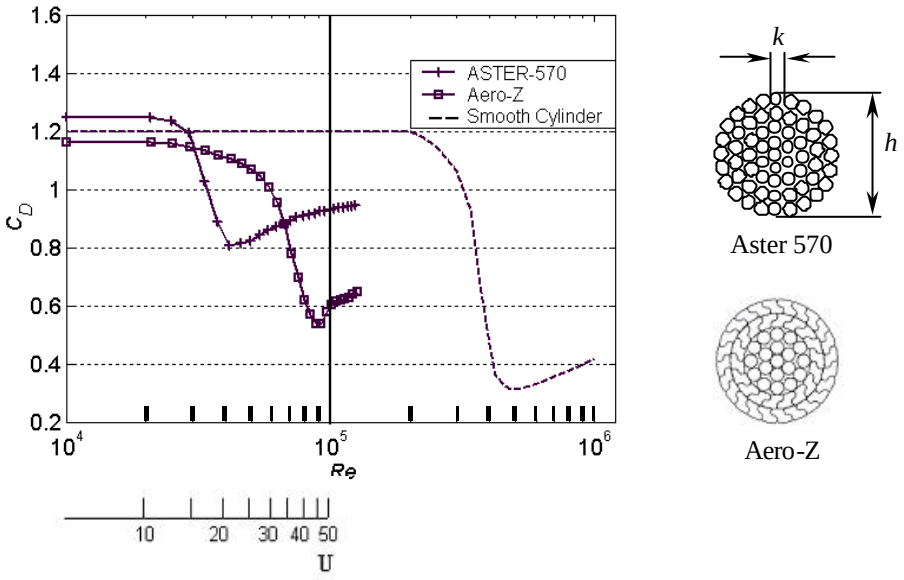

Fig. 1. C_D vs. $\mathcal{R}e$ curves for smooth and classical stranded conductors, compared to the pure cylinder. To the right the conductors' cross-sections are shown. Equivalent wind speed, shown beneath, corresponds to conductor diameters about 31 mm

3. MODEL OF WIND

In (2), the wind velocity term U is time- and space non-uniform due to the turbulence of the wind itself:

$$U(x,y,z,t) = \bar{U}(z) + u_{wind}^{fluct}(x,y,t) \tag{3}$$

Here, $\bar{U}(z)$ stands for the mean wind velocity, defined after power or logarithmic law with respect to the height over ground, z;

$u_{wind}^{fluct}(x,y,t)$ is defined after the time-dependent, spatially correlated wind fluctuations.

We should now choose between several spectral models for the wind fluctuations (Davenport, Kaimal, Von Karman, Harris, etc.) [6]. The choice may depend on which spectrum better fits the measured local wind profile[1], what regulations of local engineering code are applicable, etc. In our study we paid attention to the fact, that different spectra treat differently the characteristic scales of turbulence (if one compares Davenport to other spectra, even definitions of scales are different). In our study, three scales (alongwind, across-wind and vertical) were defined via the Counihan's empirical model [1]. Accordingly, Von Karman spectrum may be applied since it incorporates the Counihan scales explicitly:

$$\frac{w\,S(w)}{s^2} = \frac{\dfrac{w\,L_u(z)}{p\,\left\|\mathbf{U}_{wind}(z)\right\|}}{\left(1+\left(\dfrac{4.2065\,w\,L_u(z)}{p\,\left\|\mathbf{U}_{wind}(z)\right\|}\right)^2\right)^{\frac{5}{6}}} \tag{4}$$

Here,

$S(w)$ is the fluctuating component's power spectrum density ($m^2 s/rad$);

ω is the cyclic frequency of the wind fluctuation (rad/s);

U_{wind} is the mean wind velocity (m/s), being function of vertical coordinate z;

L_u is the turbulence scale (m) in the direction of the mean horizontal wind velocity, giving idea of the eddy size. In this analysis, it was defined after Counihan's model as function of vertical coordinate z and the site roughness (countryside);

s is the standard deviation of the wind velocity fluctuations (m/s).

The standard deviation s may be found by two ways, depending on available data. The first way consists in experimental definition of s after integrating the PSD of fluctuations over the frequency range. Another approach (used in our analysis) permits to directly find s from the reference wind velocity, $\|U\|_{wind}^{ref}$, and the turbulence intensity I (in percent):

$$s = I \cdot \|U\|_{wind}^{ref}. \tag{5}$$

Within the finite-element analysis, discrete samples of turbulent wind across the line span are

[1] Another option is to use the spectral model on basis of local measurements.

generated at pre-processing stage. Wind samples are then correlated spanwise via the spatial coherence function [8] with respect to the central fluctuation frequency (we used the basic eigenfrequency of the span, 0.18 Hz) and along-span (i.e., across-wind) turbulence scale.

Theoretical spectrum and the one recovered after simulation in SAMCEF/Mecano [12] are shown in Fig. 2, (a). Field of fluctuating wind across the span (Fig. 2, b) is marked by extreme fluctuation amplitudes about $\pm 15...17\ m/s$. Such level is quite comparative to some known observation data [14] about hurricanes of high turbulence intensity (in our study, I = 19 %).

In the model used by ULg, fluctuations were defined only in longitudinal direction (alongside the wind), while lateral wind non-uniformities were accounted via the spanwise correlation. However, one may also introduce the fluctuations in both remaining directions, e.g., via two additional Von Karman spectra [6]. Such an approach is used by EDF R&D group for complementary study (Fig. 2, (c)).

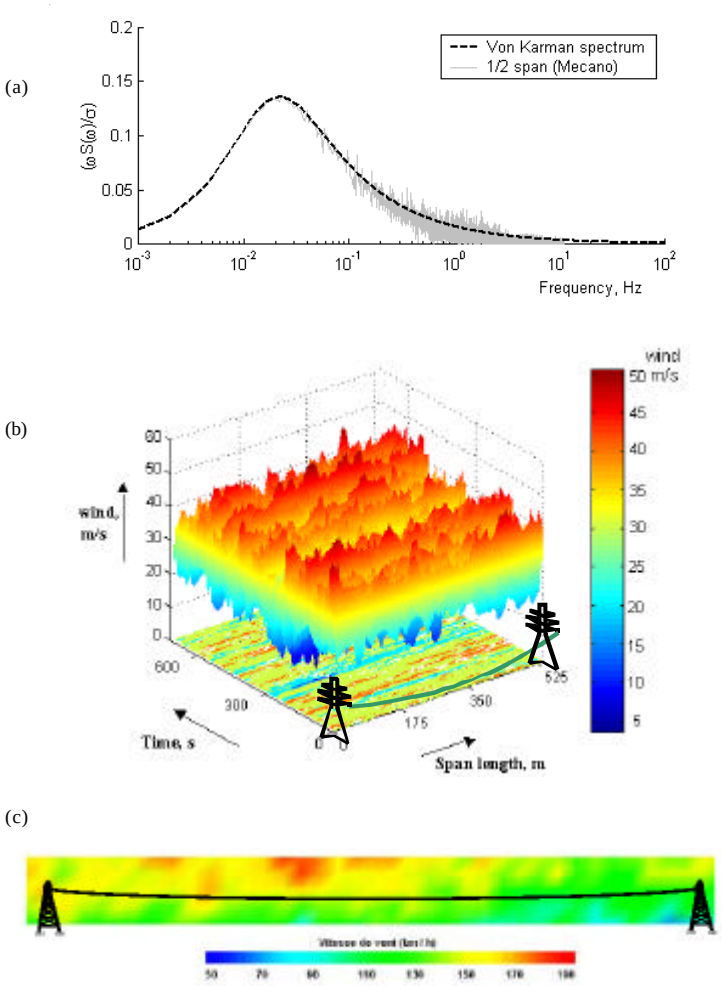

Fig. 2. Models of the fluctuating wind. (a) FFT recovery from the wind sample compared to the basic Von Karman spectrum (SAMCEF). (b) Ensemble of wind samples across the PTL span (SAMCEF). (c) Example of the transversal wind field acting on the PTL span (wind simulation toolbox developed by LCPC).

4. RESULTS

In our analysis we considered a 525 m-long span. The cable tension was 33.6 kN (for classical conductor) and 39.14 kN (for smooth conductor). With such tensions, initial sag at zero wind (16.5 m) for both types of conductors is the same.

Several analysis cases with different mean wind velocities (30 m/s and 40 m/s) were considered. Simulations were done over 10 min. interval – a duration imposed by standard recordings of wind and retained in the models of the wind fluctuations[2].

In all analysis cases, the smooth-surfaced cable was excited significantly less than the classical multistrand analogue. The tension variation (T_{max} - T_{min}) in Aero-Z is by 44 to 52 % less than in the classical cable, which means a lower risk of fatigue problems. It should be noticed, that the fatigue problem during hurricane is not related to many cycles (due to limited hurricane duration), but rather to very high amplitude of conductor movement ("oligocyclic fatigue"). In ULg analysis, the obtained displacement amplitudes of Aero-Z were by 29% to 43% less (Fig. 3, b). This relationship is confirmed in the study done independently by EDF, with the different model of wind (Fig. 2, c) and finite-element simulation tool, "Code Aster".

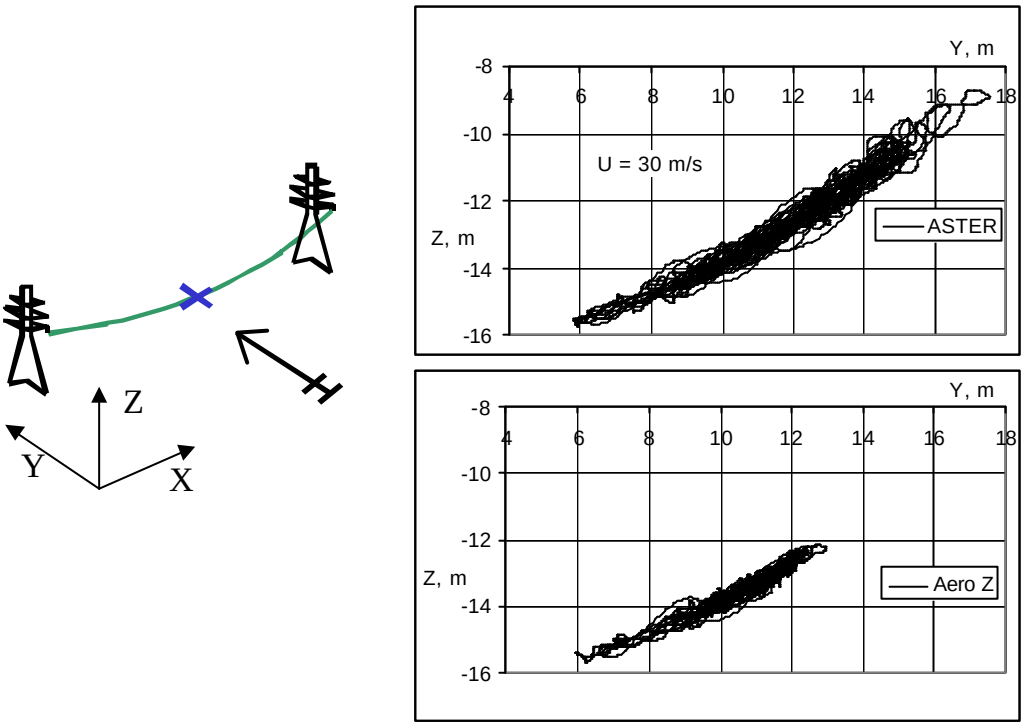

Fig. 3. Mid-point evolutions of the classical multistrand cable (above) and AERO-Z (below).
Mean wind speed: 30 m/s, alongwind turbulence scale: 200 m, turbulence intencity: 19%

For mean wind velocity $\bar{U}$=30 m/s (main analysis case), variations of the tower transverse loads ΔR_y from the smooth cable were by 34% less than from the classical analogue. This value is quite close to the results obtained independently by EDF (gain about 30%). At $\bar{U} = 40\,m/s$ variations of ΔR_y remained at the same level. In the same time, Aero-Z enjoyed especially significant gain in the mean value R_y (up to 46%).

---

[2] On current PC workstations (1.500 MHz and 64 MB of allocated RAM) single run of such analysis case took approx. 20 minutes. Basically, analysis runtime depends on the time discretization of the wind samples and the rate of problem convergence at each time step.

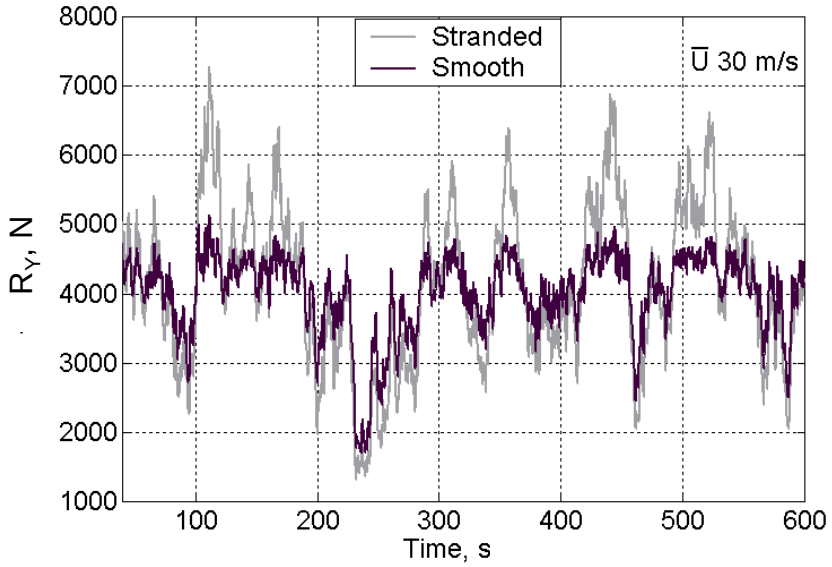

Fig. 4. Variations of the horizontal transverse load on tower end in the wind direction, R_Y, for the cable AERO-Z and the classical multistrand analogue. Mean wind velocity: 30 m/s, alongwind turbulence scale: 200 m, turbulence intencity: 19%

The reason for such gain of Aero-Z in the wind-excited response is, above all, due to its aerodynamics[3]. As the wind velocity reaches the corridor 30…40 m/s, the drag coefficient of the classical conductor, being postcritical, does not vary too much (Fig. 1). As result, the drag force (1) is free to fluctuate. Simultaneously, C_D of AERO-Z fluctuates inverse proportionally to the wind fluctuations, making the drag force quasi-constant at V between 30 and 40 m/s (Fig. 5). Thanks to such stagnation of the drag force in that velocity region, beyond the critical state the smooth cable is still much less loaded as compared to the stranded cable[4].

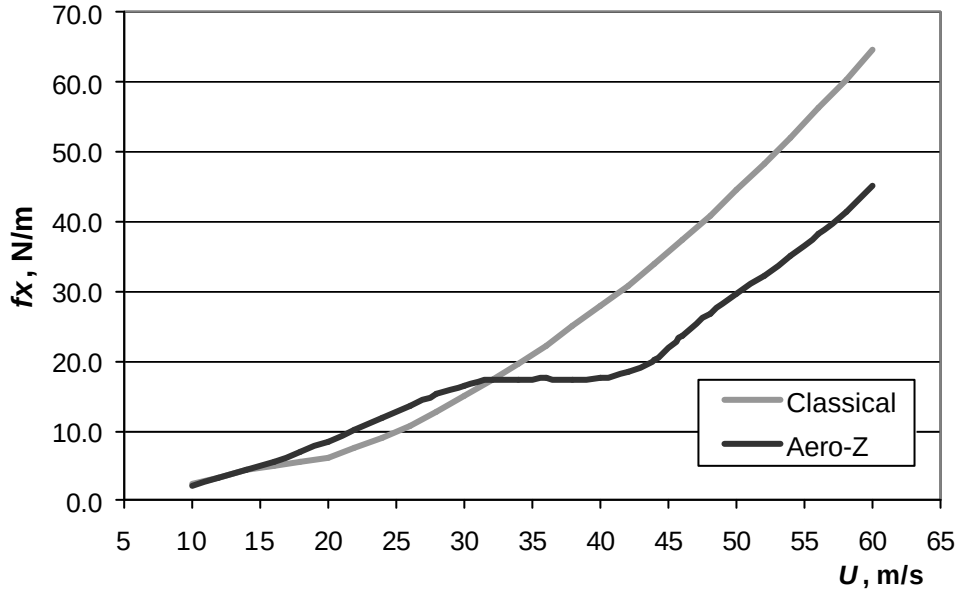

Fig. 5. Variation of drag force per unit length (1) vs. wind velocity for classical stranded and smooth (Aero-Z) conductors

[3] All other parameters, such as slightly higher inertia, although adding to the lower response on the wind fluctuations, contribute much less.

[4] For the stranded cable, the critical state occurs at lower wind velocities. However, due to smaller fall of C_D (see Fig. 1), the effect of drag force stagnation on stranded cable is not so noticeable.

An estimate of peak loads on two conductors for different mean wind velocities was then done. The maximum transversal forces, plotted against mean wind velocities ranging from 2 up to 35 m/s, may be compared to the curves of PTL span loading as specified by codes CEI 60826 and CENELEC 50341, see Fig. 6.

Both codes rely on spectral analysis models, while the drag coefficients are assumed to be invariant ($C_D \approx 1$). When accounting actual drag characteristic, the classical conductor (ASTER) does fit the code-divided dependencies quite well (mainly because of its "shallow" drag crisis, see Fig. 1). Contrary to that, Aero-Z curve makes it clear, that both standards overestimate the loading on this smooth conductor for high wind velocities. For regular mean wind velocities (20 m/s or less), loads of smooth conductor are similar, or a bit higher, than the loads on stranded conductor.

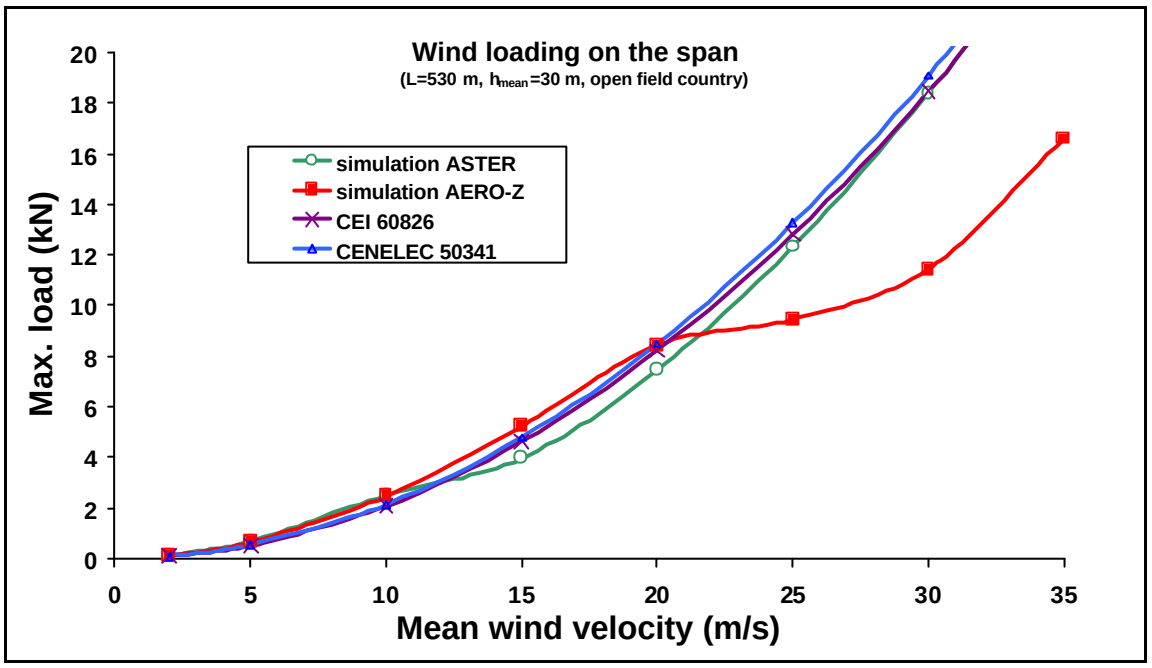

Fig. 6. Maximum aerodynamic forces acting on the 530 m long span plotted against the mean wind velocity on reference height 10 m

5. CONCLUSION

In present study, both qualitative and quantitative estimates of the effect of low drag cable in extreme conditions were done. The study makes it clear, that these differences influence the conductor loading in such a degree that the inherent loads to supporting structures may, in turn, depend quite significantly on appropriate conductor type.

Our analysis has confirmed theoretical and wind tunnel experimental estimations about effectiveness of some smooth conductors in the hurricane wind conditions. The significant reduction in dynamic response of AERO-Z, compared to the classical stranded cable, is due to its low-drag properties. Such conductor imposes lower loads (up to –40%) on other PTL components (pylons, insulators etc.) for high wind velocities and should be less susceptible to fatigue effects.

In their estimation of loads on the span, codes CEI 60826 and CENELEC 5034 do not take into account the flow- and roughness – specific differences in aerodynamic properties

between the stranded and smooth conductors. This simplification may be considered as tolerable for the stranded conductors. However, in case of smooth conductors like Aero-Z, ignoring the aerodynamic specifics may introduce a significant overestimation in the code prediction of span loading under hurricane winds.

6. ACKNOWLEDGMENTS

Authors thank Dr. Daniel Guéry (Nexans) and Mrs Laure Pellet (EDF) for their valuable input in the present studies.
This work has been partially supported by European project IMAC G1RD-CT2000-00460.

7. REFERENCES

[1] Simiu, E., Scanlan, R. H.: „Wind Effects on Structures: Fundamentals and Applications to Design", *J.Wiley & Sons*, 1996

[2] Scruton, C., Rogers, E. W. E., "Wind Effects on Buildings and Other Structures: Steady and Unsteady Wind Loadings on Buildings and Structures", Phil. Trans. Roy. Soc., London, Series A v. 269 (1971).

[3] Davenport, A.: „The Dynamics of Cables in Wind", *¨Proc. of Int. Symp. on Cable Dynamics*, Liège, Belgium, 1995

[5] Cardona, A. : „ An Integrated Approach to Mechanism Analysis", PhD Thesis, *Collection des Publications de la Faculté des Sciences Appliquées de l'Université de Liège n° 127*, 1989

[6] Guillin, A., Cremona C. : „Développement d'algorithmes de simulation de champs de vitesse du vent", éd. *Laboratoire Central des Ponts et Chaussées-France*, 1997

[7] Cremona C., Foucriat, J-C.: „Comportement au Vent des Ponts", *Presses de l'Ec. Nat. des Ponts et Chaussées*, 2002

[8] Keutgen, R. : „Galloping Phenomena: Finite Element Approach", PhD Thesis, *Collection des Publications de la Faculté des Sciences Appliquées de l'Université de Liège n° 193*, 1999

[9] Miyata et al., «On aerodynamically stable PE-stay-cables with increased drag force», *Proc. Cable Dynamics Symp.*, pp. 481-488, Liege, 1995

[10] Zdravkovich, M. M., «Flow Around Circular Cylinders», vol. I, *Oxford University Press*, 1997

[11] Davenport, A., "How can we simplify and generalize wind loads?", *J. Wind Eng. & Ind. Aerodyn.* vol. 54/55, pp. 657-669 (1995)

[12] SAMCEF v. 10 – a general-purpose FEA software, *by SAMTECH S.A.,* rue des Chasseurs-Ardennais, 8, B-4031 Angleur-Liege, Belgium

[13] Miller, C., "A once in 50-year wind velocity map for Europe derived from mean sea level pressure measurements", *J. Wind Eng.& Ind. Aerodyn.* vol. 91 pp. 1813–1826 (2003)

[14] Schroeder, J. L., Smith, D. A., "Hurricane Bonnie wind ?ow characteristics as determined from WEMITE", *J. Wind Eng.& Ind. Aerodyn.* vol. 91 pp. 767–789 (2003)